The 4th European sCO_2 Conference for Energy Systems
March 23-24, 2021, Online Conference

2021-sCO2.eu-113

AN ATTEMPT FOR ESTABLISHING PRESSURE RATIO PERFORMANCE MAPS FOR SUPERCRITICAL CARBON DIOXIDE COMPRESSORS IN POWER APPLICATIONS

Ihab Abd El Hussein *
University of Duisburg-Essen
Duisburg, Germany
ihab.abd-el-hussein@uni-due.de

Sebastian Schuster
University of Duisburg-Essen
Duisburg, Germany

Dieter Brillert
University of Duisburg-Essen
Duisburg, Germany

ABSTRACT

Carbon dioxide in the supercritical state (sCO_2) has drawn much interest lately. It is considered as a promising fluid for next-gen power plants with many researchers investigating this technology. Cycle simulation and control requires compressor performance maps valid for variable inlet conditions. In this paper, an attempt is made for establishing a pressure ratio based performance map for sCO_2 compressors in power applications. For that purpose the so-called Glassman approach is considered. This model has been originally established for fluids obeying the ideal gas law. Therefore, a modification is proposed to take into consideration the real gas equation of state and to allow wide variation of the isentropic volume exponent k_v. Computational fluid dynamics (CFD) is used to predict the performance of a single stage radial compressor. Results for different k_v values at the compressor inlet confirms the validity of the proposed model with both the polytropic efficiency and the reduced enthalpy deviations limited to 1 percent. On the other hand, predicted pressure ratio shows difference of around 3 percent from k_v=7.1 to k_v= 4.1. A further decrease of k_v to 2.5 extends the difference up to 8 percent.

INTRODUCTION

With the increased environmental concerns and awareness regarding the global warming, renewable resources are gaining higher shares in the energy sector. These technologies have high intermittency in the power production and therefore, conventional fossil power plants are required to operate with high flexibility to balance these fluctuations.

Carbon dioxide in the supercritical state (sCO_2) has drawn much interest lately as an alternative fluid for next-gen power plants with many researcher investigating this technology. Especially in the so-called liquid-like region, sCO_2 is characterized by high density (0.5 to 0.7 of liquid water) and low viscosity (~ air). These properties among others promise small components with reduced losses and consequently cycles with high flexibility and efficiency.

Cycle control and simulation requires reliable performance prediction of the compressor at variable inlet conditions. This can be done using for instance a mean-line model [2]. Though, such models requires validity and accuracy of the underlying loss estimation at variable inlet conditions. Alternatively, compressor performance map with reduced values are widely implemented for such purpose. For that, the compressor performance at a reference condition should be known, experimentally measured for example. This approach can ensure high prediction accuracy of the performance from a reference inlet condition to another given the validity of the applied formulation. In fact, most formulations are only valid for a constant isentropic exponent. However, this is not true for typical sCO_2 compressor inlet conditions (Fig. 1).

The isentropic volume exponent k_v is defined as [1]:

$$k_v = -\frac{v}{p} \cdot \frac{c_p}{c_v} \cdot \left(\frac{\partial p}{\partial v}\right)_T \qquad (1)$$

For fluids obeying the ideal gas law, k_v reduces to the specific heat ratio which is also known as the isentropic exponent in such cases. Figure 1 illustrates k_v range for typical sCO_2 compressors inlet conditions.

To cope with its high variation for sCO_2, Barber Nichols Inc. adopted a formulation based on the work by Glassman [3]. Comparison of the results against experimental measurements showed good matching regarding the enthalpy change, yet efficiency predictions show up to 20 percent deviation from experimental data [4]. In a similar context, Jeong et al. [5] studied several formulations of the reduced maps and compared the results to experimental measurements and numerical results. In their study, where the specific heat ratio is used as the

* corresponding author(s)

DOI: 10.17185/duepublico/73954

isentropic exponent, none of the formulations was able to consistently predict the pressure ratio, efficiency or the enthalpy change. Moreover, Pham et al. [6] considered the conventional Mach number similarity, their study shows good prediction accuracy regarding the reduced enthalpy and efficiency of sCO_2 compressors with k_v ranging from 4.5 to 14 at its inlet. On the other hand, due to the wide range of k_v, the pressure ratio varied substantially and therefore a corrected pressure ratio instead of the actual one is proposed.

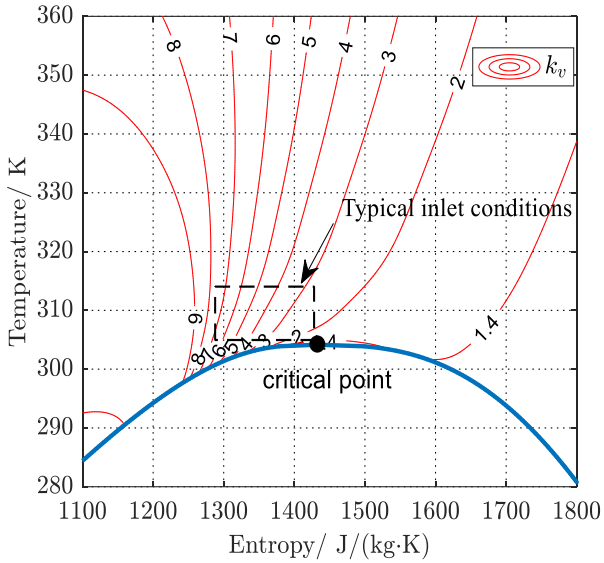

Figure 1: Variation of the isentropic volume exponent k_v with typical sCO_2 compressors inlet conditions

In this paper, an attempt is made to establish compressor map based on the pressure ratio for sCO_2 compressors. Such map would facilitate the cycle control and simulation by providing direct relation with a measured parameter (pressure).

UNDERLYING THEORY

The Buckingham Π-theorem [7] represents the foundation for the similarity analysis. For geometrically similar machines, the compressor performance can be related to four independent parameters:

$$(\eta, \pi, \Delta h) = f\left(\underbrace{\frac{\dot{m}}{\rho_{0t} \cdot a_{0t} \cdot D_2^2}}_{\dot{m}_{red}}, \underbrace{\frac{N \cdot D_2}{a_{0t}}}_{N_{red}}, \underbrace{\frac{\rho_{0t} \cdot N \cdot D_2 \cdot b_2}{\mu_{0t}}}_{Re}, k_v\right) \quad (2)$$

Representing the reduced mass flow, reduced speed, Reynolds number and the isentropic exponent. By considering an isentropic compression process for a radially bladed impeller, the pressure ratio π can be related to the isentropic exponent k_v (Eq. 3).

$$\pi = [M_{u2}^2 \cdot (k_v - 1) + 1]^{\frac{k_v}{k_v - 1}} \quad (3)$$

With M_{u2} being the circumferential Mach number. For constant M_{u2} according to the Mach number similarity, π has a high dependence on the k_v value.

Alternatively, by considering a proportionality of the reduced speed with the critical velocity (Eq. 4), the dependence of π on k_v can be minimized.

$$N_{red} = \frac{N \cdot D_2}{a_{0t}} \propto \frac{N \cdot D_2}{v_{cr}} \quad (4)$$

The critical velocity is defined as the sonic speed once the flow is brought isentropically to Mach number equal 1 (Eq. 5) from the inlet total pressure p_{0t} and total temperature T_{0t} while assuming a constant k_v value obtained from the inlet conditions.

$$v_{cr} = \sqrt{\frac{2 \cdot k_v}{k_v + 1} \cdot Z_{0t} \cdot R \cdot T_{0t}} \quad (5)$$

With Z, being the compressibility factor and R, being the gas constant. Accordingly, the pressure ratio can be estimated for an isentropic compression following Eq. 6.

$$\pi = \left[2 \cdot C \cdot \frac{k_v - 1}{k_v + 1} + 1\right]^{\frac{k_v}{k_v - 1}} \quad (6)$$

With $C=\Delta h/v_{cr}^2$. Figure 2 compares the pressure ratio using Eq.3 and Eq. 6.

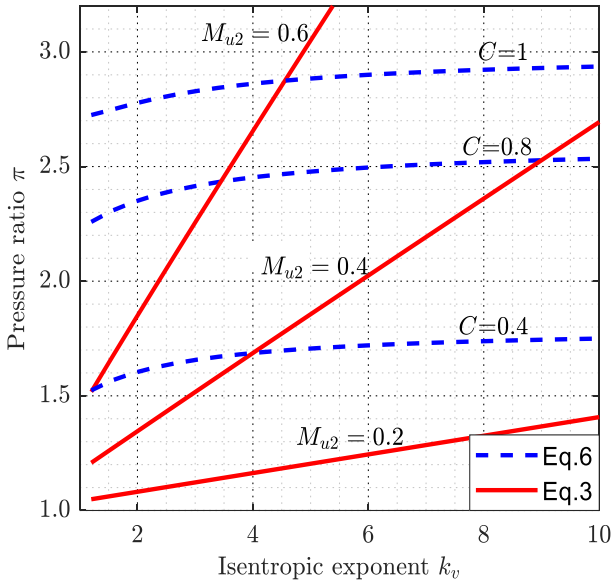

Figure 2: Dependence of the pressure ratio on k_v value for Mach number similarity and critical velocity proportionality

For the range of interest (k_v around 3 to 7), adoption of the rotational speed proportionality to the critical velocity results in

small variations of the pressure ratio. This is in contrast to the conventional Mach number similarity where the deviation is very high especially as M_{u2} increases.

Similar proportionality can be considered from the reduced mass (Eq. 7)

$$\dot{m}_{red} = \frac{\dot{m}}{\rho_{0t} \cdot a_{0t} \cdot D_2^2} \propto \frac{c_m}{a_{0t}} \propto \frac{c_m}{v_{cr}} \tag{7}$$

In the original approach, Glassman assumes this proportionality to be equivalent to the ratio of the reduced mass flow to the reduced mass flow at choke condition. With the latter being only a function of the isentropic exponent [3]. Similar interpretation for considering the effect of k_v on the reduced mass flow is followed in the work of Roberts and Soljander [8]. Nevertheless, this assumption neglects the fact that the ratio of the density at the critical condition to the density at the total condition differs substantially with the k_v value (Fig. 3).

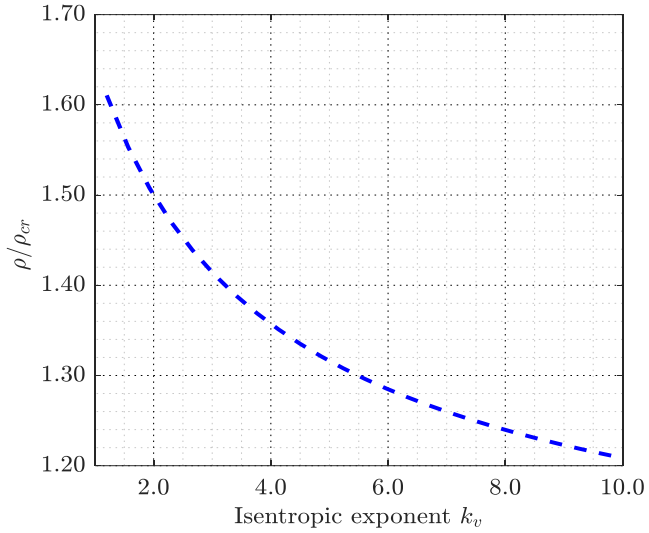

Figure 3: Ratio of the density to critical density with respect to k_v

In this work, the reduced mass flow rate is modified in comparison to the original Glassman approach, where the mass flow rate is reduced by the mass flow rate at critical velocity and total density. This produces, with the reduced speed (Eq. 4), the typical inlet flow coefficient (Eq.8).

$$\frac{\dot{m}}{\rho_{0t} \cdot v_{cr} \cdot D_2^2} \propto \frac{c_{m1}}{u_2} \tag{8}$$

Moreover, an additional term is added to match volume flow ratio across the compressor. Analogous to ideal gas process, the polytropic work of a real gas is approximated following Eq. 9

$$y = \frac{n}{n-1} \cdot Z_0 \cdot R \cdot T_0 \cdot (\pi^{\frac{n-1}{n}} - 1) \tag{9}$$

With n being the polytropic exponent (pv^n=constant) that might be estimated using the compressor inlet and outlet properties. This is used to estimate the volume flow ratio (Eq. 10)

$$\sigma = \frac{\dot{V}_4}{\dot{V}_0} = \pi^{\frac{-1}{n}} = \left(2 \cdot C \cdot \eta \cdot \frac{k_v}{k_v + 1} \cdot \frac{n-1}{n} + 1\right)^{\frac{-1}{n-1}} \tag{10}$$

Consequently, the reduced mass considered in this work reads as follows:

$$\dot{m}_{red} = \frac{\dot{m} \cdot \sigma}{\rho_{0t} \cdot v_{cr} \cdot D_2^2} \tag{11}$$

METHODOLOGY

This work utilizes computational fluid dynamics (CFD) to study the accuracy of pressure ratio based performance maps. This is due to the limited available experimental data for sCO_2 compressors that are coupled with high uncertainty regarding the enthalpy change and the efficiency that limits the quantitative comparison.

A single stage radial compressor is considered for the study. The compressor design is generated using an in-house design tool for sCO_2 compressors [9]. Figure 4 illustrates a frontal view of the three dimensional impeller that features typical radial machine geometry with a specific speed and specific diameter of 0.23 and 4.5, respectively. The impeller has a slightly backward curved blade with β_2=105° from tangential direction. Downstream the impeller, a vaneless diffuser followed by a rectangular volute are implemented.

CFD simulations are conducted using the steady RANS solver of the commercial CFD code CFX 18 coupled with the SST turbulence model and the wall function in order to reduce the computational effort. Moreover, from a base mesh for a single passage, doubling the nodes number to around 500,000 resulted in approximately 0.5 efficiency point difference, an another doubling of the nodes number resulted in a mere 0.05 efficiency point variation. Similarly, from a base mesh for the volute, increasing the mesh size to around 1 million nodes resulted in 1 efficiency point variation, while a further increase of the mesh size by around 1.6 factor produced only 0.02 efficiency point difference. Therefore, around 500,000 nodes and 1 million nodes for a single passage and for the volute, respectively, are considered to provide mesh independent results. Furthermore, fluid properties for sCO2 are implemented through real gas tables calculated using the Span and Wagner equation of state [10] from the NIST Refprop database [11]. The real gas tables have a resolution of around 0.1 K for the temperature and around 0.22 bar for the pressure which is found to provide independent results. Simulations are considered converged when all the following criteria are met: RMS residuals fall below $1e^{-4}$, imbalance is less than 0.1 percent in all domains and constant or small variation of the enthalpy change within less than 0.2 percent. Assessment of the adopted numerical approach has been previously done using pressure ratio measurement of a sCO_2 compressor running near the critical point [12].

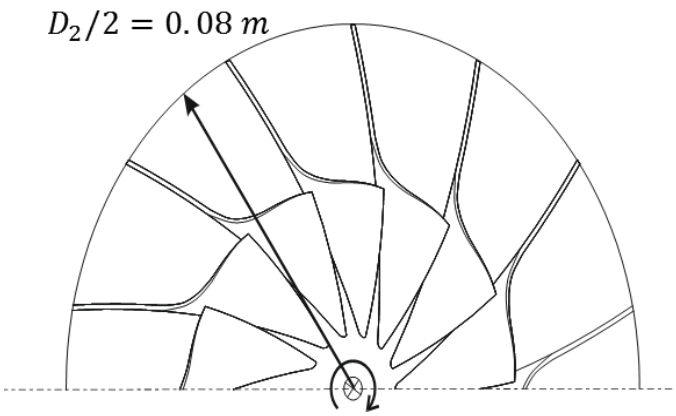

Figure 4: Frontal view of the impeller

Three inlet conditions at 318 K and 140 bar, 110 bar and 100 bar are selected for the simulations with k_v values of 2.5, 4.1 and 7.1, respectively. Additionally, selected inlet conditions have density values ranging from around 500 to 720 kg/m^3 such that they are representative of the region of interest. Simulations are limited to one-phase flow and the location of the inlet conditions provided adequate distance from the two-phase region.

RESULTS

The simulations are conducted for a pressure ratio of around 2.2. From the properties at the different inlet conditions, the critical velocity is calculated and accordingly the rotational speed is found. This results in a circumferential Mach number M_{u2} variation from 0.5 to 0.76 with the value increasing for lower k_v value. In contrast, variation of the rotational speed is limited from around 22100 rpm to around 20300 rpm showing less than ten percent variation. In comparison, a Mach number similarity requires much larger rotational speed variation of around 60 percent for the considered inlet conditions. Moreover, given the small variation of rotational speed, Reynolds number variation is limited to a ratio less than 1.1. Therefore, correction for the effect of *Re* variation is considered unnecessary. Moreover, evaluation of σ term in the mass flow parameter (Eq.11) is done by considering constant values for C=0.76 and η=0.9 while n is a constant value for each inlet condition being a function of k_v and η. This is done in order to reduce the implicit nature of the mass flow parameter on the performance value and thus to promote the simplicity of the model implementation.

Figure 5 illustrates the predicted stage total polytropic efficiency (Eq. 12) in terms of the reduced mass flow rate for the different inlet conditions.

$$\eta_t = \frac{y_t}{\Delta h_t} \qquad (12)$$

With y_t being the total polytropic work and Δh_t being the total enthalpy change. Considering k_v=4.1 as reference condition, an overall good matching of the stage polytropic efficiency is found in comparison with the other k_v values. Exception is observed for reduced mass flow rates lower than its Best efficiency point (BEP), where high deviation between result for k_v=2.5 and the other two inlet conditions takes place. At this region, the efficiency experience high gradients with respect to the mass flow rate parameter. This is found to be a result of high recirculation and incidence losses at this region (Fig. 7). Therefore, the difference is thought to originate from the effect of the difference in the inlet flow coefficient which is around 6 percent higher for k_v=2.5 in comparison to k_v=4.1. Nevertheless, this is considered as a special case for the studied compressor that has a very small blade angle at the shroud. This leads to high recirculation losses at small inlet flow coefficient.

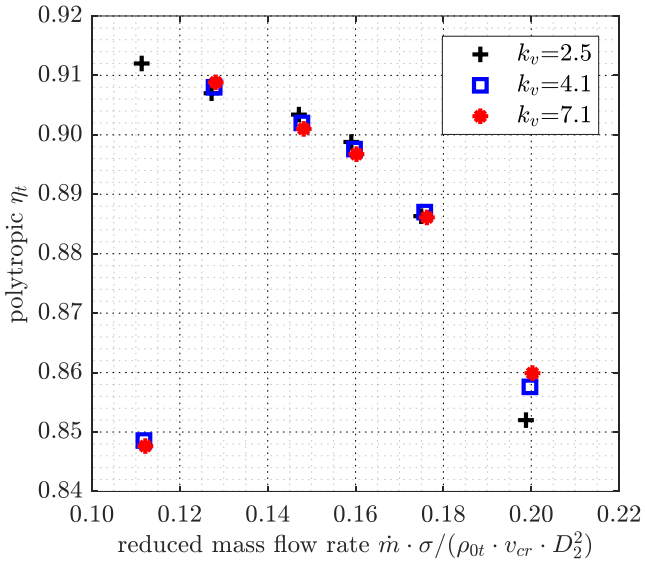

Figure 5: Variation of the stage total polytropic efficiency with respect to the reduced mass flow rate with k_v

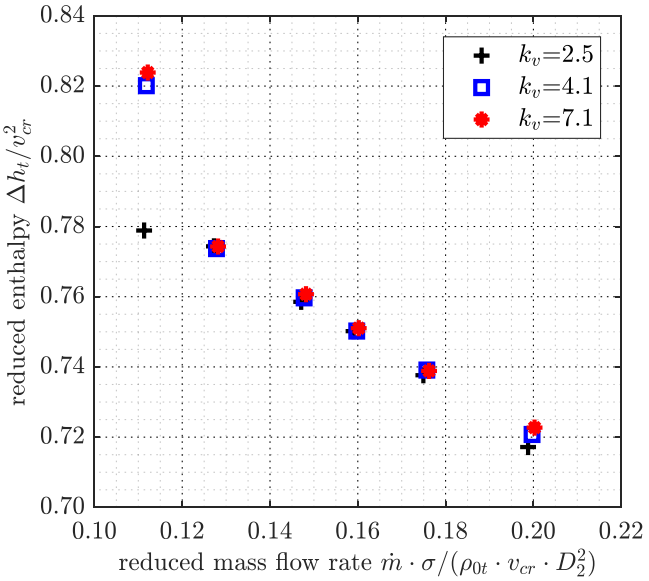

Figure 6: Variation of the reduced enthalpy change with respect to the reduced mass flow rate with k_v

A similar result is found regarding the reduced enthalpy change (Fig. 6) with a very good matching of the results for different k_v values. Left to the BEP of k_v=4.1, an exception to this matching is found which is related to the flow recirculation that causes distortion of the flow direction and consequently impacting the enthalpy change.

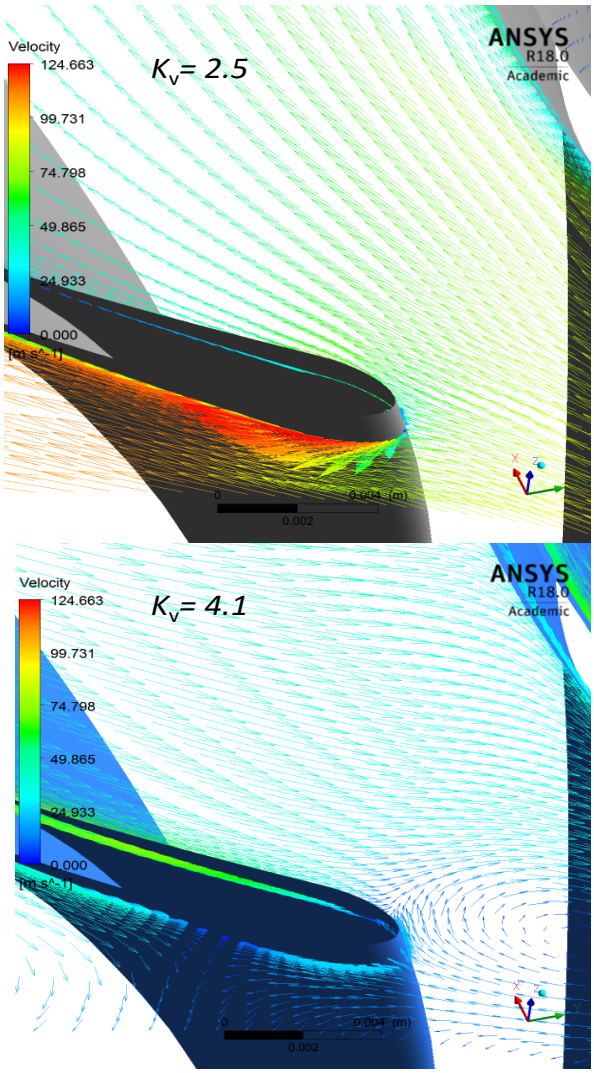

Figure 7: velocity vector at the rotor inlet at a constant span location of 0.95 for k_v =2.5 and k_v =4.1

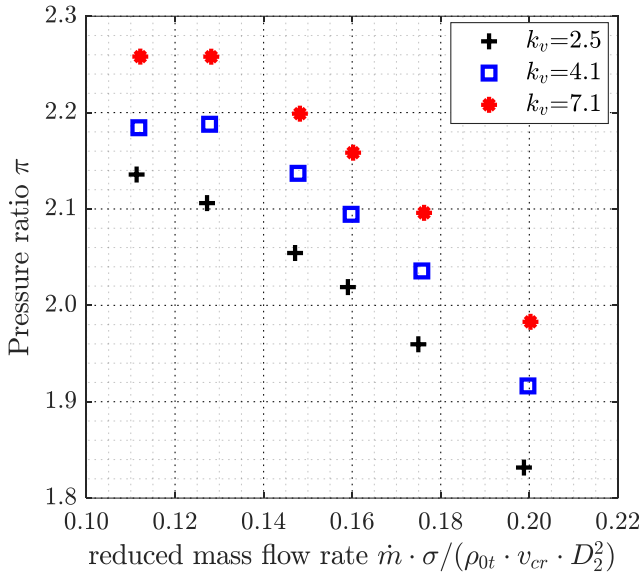

Figure 8: Predicted pressure ratio at constant reduced speed for different k_v values

The main attempt of this work is to establish pressure ratio based performance maps for sCO2 compressors. Figure 8 depicts the predicted pressure ratio for the different k_v values. Due to the slight backward curvature of the blade outlet angle, predicted pressure ratio of each k_v line shows small reduction with respect to the reduced mass flow parameter. Results however, show a consistent deviation limited to around 3 percent between the cases with k_v=7.1 and k_v=4.1. A further decrease of the k_v to 2.5 increased the pressure ratio deviation to around 8 percent. Yet, with the good matching of reduced enthalpy and the polytropic efficiency, the deviation of pressure ratio is considered a result of an inherent characteristic of this formulation as can be seen in Fig. 2 where cases having equal reduced enthalpy change but different isentropic exponent would still have different pressure ratios.

CONCLUSION

In this paper, an attempt is made to establish pressure ratio based performance maps for sCO_2 compressors. For that purpose, the so-called Glassman approach is used in order to account for the effect of the isentropic exponent variation on the pressure ratio. A modification of the original mass flow parameter is introduced to account for the ratio of the inlet density to the critical density. Moreover, an additional term is also introduced that considers the effect of k_v of the volume flow ratio across the stage.

Validation of the model is conducted against CFD simulations of a single stage radial compressor with three k_v values of 2.5, 4.1 and 7.1 at the inlet. Results show good matching of the reduced enthalpy and the stage total polytropic efficiency with less than 1 percent deviation. Exception is found for small reduced mass flow rate, where recirculation and incidence losses that are dependent on the inlet velocity triangle

took place. The predicted pressure ratio shows a difference of around 3 percent between the case with k_v=7.1 and k_v=4.1. A further decrease of k_v to 2.5 widened the difference to around 8 percent.

Moreover, for the considered inlet condition and pressure ratio, the M_{u2} value varied from around 0.5 to around 0.75 in an inverse relation with k_v. At higher M_{u2} values shock losses might take place which can affect the validity of the model. Similarly, maximum variation of the inlet flow coefficient is around 10 percent between the studied cases. Depending on the considered compressor and its performance characteristic (efficiency variation with respect to mass flow rate), more conservative limit might be used especially in region where high variation of the efficiency take place as at low inlet flow coefficient in the studied compressor.

NOMENCLATURE

a	Sonic speed	m/s
b_2	Impeller exit width	m
c	Absolute velocity	m/s
C	Constant = $\Delta h/v_{cr}^2$	-
c_p	Specific heat capacity const. pressure	J/(kg · K)
c_v	Specific heat capacity const. volume	J/(kg · K)
D_2	Impeller diameter	m
h	Specific enthalpy	J/kg
s	Specific entropy	J/(kg · K)
k	Ideal gas isentropic exponent	-
k_v	Isentropic volume exponent	-
$\dot{m}$	Mass flow rate	kg/s
M_{u2}	Circumferential Mach number	-
N	Rotational speed	s^{-1}
n	Polytropic exponent	-
p	Pressure	Pa
R	Gas constant	J/(kg · K)
T	Temperature	K
u_2	Impeller tip speed	m/s
$\dot{V}$	Volumetric flow rate	m^3/s
v	Specific volume	m^3/kg
v_{cr}	Critical velocity	m/s
y	Polytropic work	J/kg
Z	Compressibility factor	-
	Greek letter	
η	Polytropic efficiency	-
ρ	Density	kg/m^3
ρ_{cr}	Critical density	kg/m^3
π	Pressure ratio	-
μ	Dynamic viscosity	Pa·s
σ	Mass flow correction factor	-
	Subscript	
m	Meridional component	
red	Reduced value	
t	Total condition	
0	Stage inlet	
2	Impeller tip	
4	Stage exit	

ACKNOWLEDGEMENTS

The work leading to these results has received funding from the European Union under grant agreement number 764690 for the sCO2-Flex project under the HORIZON 2020 program.

REFERENCES

[1] Kouremenos D. A., and Antonopoulos K. A. (1987). Isentropic exponents of real gases and application for the air at temperatures from 150 K to 450 K, Acta Mechanica, **65**(1-4), pp. 81–99.

[2] Romei A., Gaetani P., Giostri A., and Persico G. (2020). The Role of Turbomachinery Performance in the Optimization of Supercritical Carbon Dioxide Power Systems, Journal of Turbomachinery, **142**(7), p. 1187.

[3] Glassman A. J. (1972). Turbine Design and Application, NASA SP_290_VOL1-3,pp 57-60.

[4] Wright s. A., Radel R. F., Venom M. E., Rochau G. E., and Pickard P. S. (2010). Operation and Analysis of a supercritical CO2 Brayton Cycle: SANDIA REPORT SAND2010-0171.

[5] Jeong Y., Son S., Cho S. k., Baik S., and Lee J. I. (2019). A Comparison Study for Off-Design Performance Prediction of a Supercritical CO2 Compressor With Similitude Analysis, Volume 3A: Fluid Applications and Systems, American Society of Mechanical Engineers.

[6] Pham H. S., Alpy N., Ferrasse J. H., Boutin O., Tothill M., Quenaut J., Gastaldi O., Cadiou T., and Saez M. (2016). An approach for establishing the performance maps of the sc-CO2 compressor: Development and qualification by means of CFD simulations, International Journal of Heat and Fluid Flow, **61**, pp. 379–394.

[7] Buckingham E. (1914). On Physically Similar Systems; Illustrations of the Use of Dimensional Equations, Phys. Rev., **4**(4), pp. 345–376.

[8] Roberts S. K., and Sjolander S. A. (2005). Effect of the Specific Heat Ratio on the Aerodynamic Performance of Turbomachinery, Journal of Turbomachinery, **127**(4), pp. 773–780.

[9] Abd El Hussein I., Hacks A. J., Schuster S., and Brillert D. (2020). A Design Tool for Supercritical CO2 Radial Compressors based on the Two-Zone Model. ASME, Turbomachinery Technical Conference & Exposition, September 21 – 25, 2020.

[10] Span R., and Wagner W. (1996). A New Equation of State for Carbon Dioxide Covering the Fluid Region from the Triple-Point Temperature to 1100 K at Pressures up to 800 MPa, Journal of Physical and Chemical Reference Data, **25**(6), pp. 1509–1596.

[11] Lemmon E. NIST Reference Fluid Thermodynamic and Transport Properties Database: Version 9.0, NIST Standard Reference Database 23.
[12] Hacks A. J., Schuster S., and Brillert D. (2019). Stabilizing Effects of Supercritical CO2 Fluid Properties on Compressor Operation†, IJTPP, **4**(3), p. 20.

DOI: 10.17185/duepublico/73954
URN: urn:nbn:de:hbz:464-20210330-100643-6